



Supplement of

Assessing the simulated soil hydrothermal regime of the active layer from the Noah-MP land surface model (v1.1) in the permafrost regions of the Qinghai-Tibet Plateau

Xiangfei Li et al.

Correspondence to: Tonghua Wu (thuawu@lzb.ac.cn)

The copyright of individual parts of the supplement might differ from the article licence.

The soil hydraulic parameters of each layer, including the porosity (θ_s), saturated hydraulic conductivity (K_s), hydraulic potential (ψ_s), the Clapp-Hornberger parameter (b), field capacity (θ_{ref}), wilt point (θ_w), and saturated soil water diffusivity (D_s), were determined using the pedotransfer functions proposed by Hillel (1980), Cosby et al. (1984), and Wetzel and Chang (1987):

$$\theta_s = 0.489 - 0.00126(\%sand) \quad (S1)$$

$$K_s = 7.0556 \times 10^{-6.884+0.0153(\%sand)} \quad (S2)$$

$$\psi_s = -0.01 \times 10^{1.88-0.0131(\%sand)} \quad (S3)$$

$$b = 2.91 + 0.159(\%clay) \quad (S4)$$

$$\theta_{ref} = \theta_s \left[\frac{1}{3} + \frac{2}{3} \left(\frac{5.79 \times 10^{-9}}{K_s} \right)^{1/(2b+3)} \right] \quad (S5)$$

$$\theta_w = 0.5\theta_s \left(\frac{-200}{\psi_s} \right)^{-1/b} \quad (S6)$$

$$D_s = b \cdot K_s \cdot \left(\frac{\psi_s}{\theta_s} \right) \quad (S7)$$

where $\%sand$ and $\%clay$ represent the percentage (%) of sand and clay content in soil, respectively.

Table S1 Soil discretization scheme and soil particle fraction in this study.

Layer	Z_i	ΔZ_i	$Z_{h,i}$	Sand (%)	Silt (%)	Clay (%)
1	0.010	0.020	0.020	85.48	12.59	1.93
2	0.040	0.040	0.060			
3	0.090	0.060	0.120			
4	0.160	0.080	0.200			
5	0.260	0.120	0.320	81.15	15.58	3.27
6	0.400	0.160	0.480	86.62	11.16	2.22
7	0.580	0.200	0.680	78.73	18.06	3.21
8	0.800	0.240	0.920	88.12	8.98	2.90
9	1.060	0.280	1.200	95.00	3.00	2.00
10	1.360	0.320	1.520			
11	1.700	0.360	1.880			
12	2.080	0.400	2.280			
13	2.500	0.440	2.720	90.00	5.00	5.00
14	2.990	0.540	3.260			
15	3.580	0.640	3.900			
16	4.270	0.740	4.640			
17	5.060	0.840	5.480	68.00	20.00	12.00
18	5.950	0.940	6.420			
19	6.940	1.040	7.460			
20	7.980	1.040	8.500			

Layer node depth (Z_i), thickness (ΔZ_i), and depth at layer interface ($Z_{h,i}$) for default soil column.

All in meters.

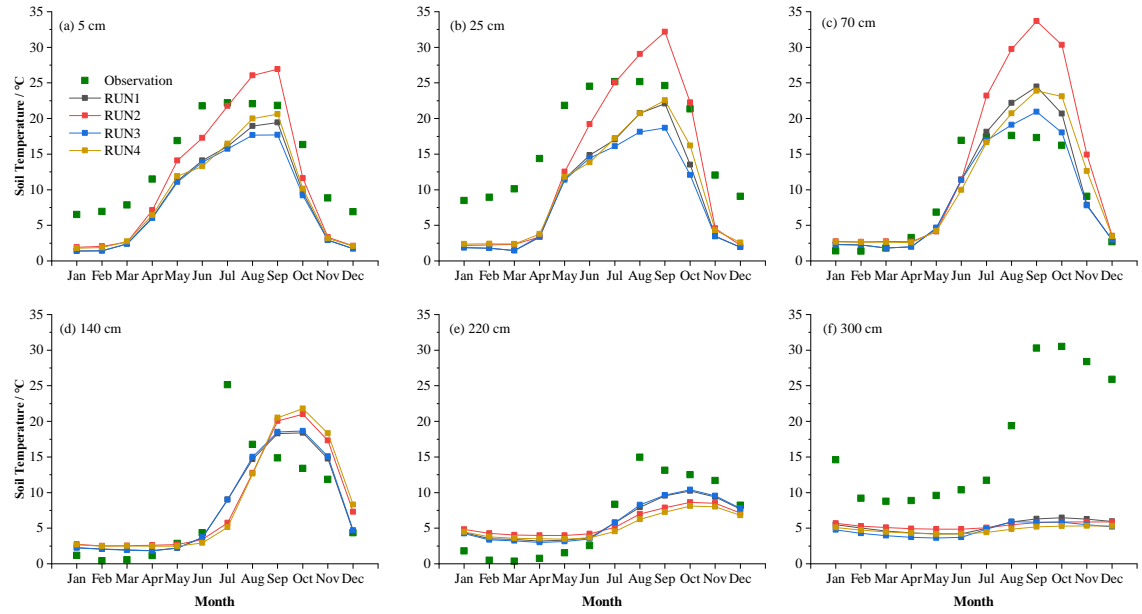


Figure. S1 Monthly soil liquid water (SLW in %) at (a) 5 cm, (b) 25 cm, (c) 70 cm, (d) 140 cm, (e) 220 cm, (f) 300 cm for the RUN process.

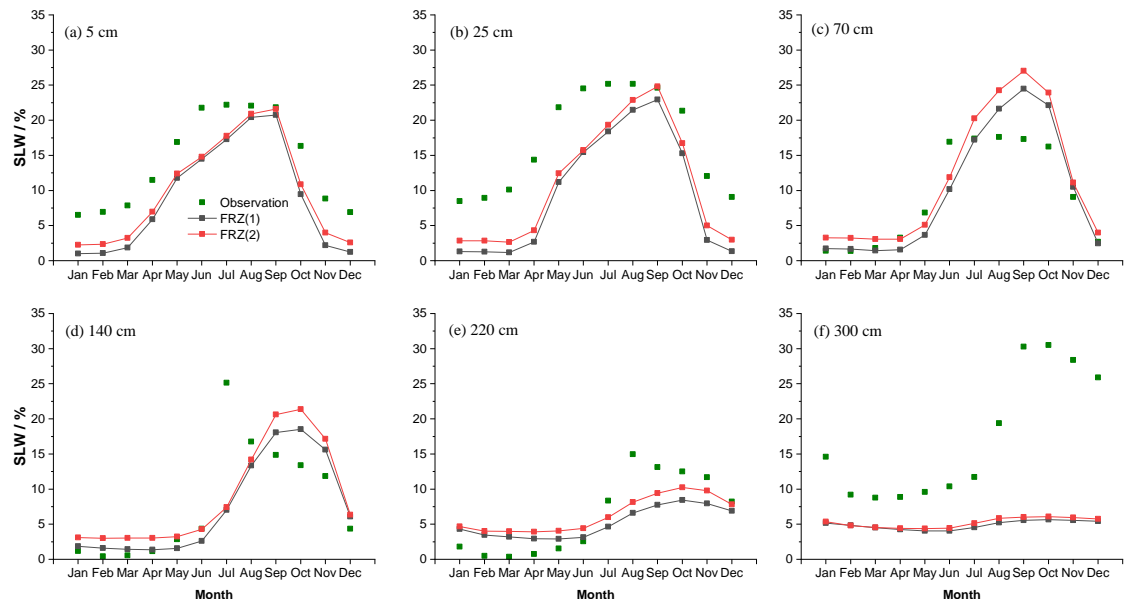


Figure. S2 Monthly soil liquid water (SLW in %) at (a) 5 cm, (b) 25 cm, (c) 70 cm, (d) 140 cm, (e) 220 cm, (f) 300 cm for the FRZ process.

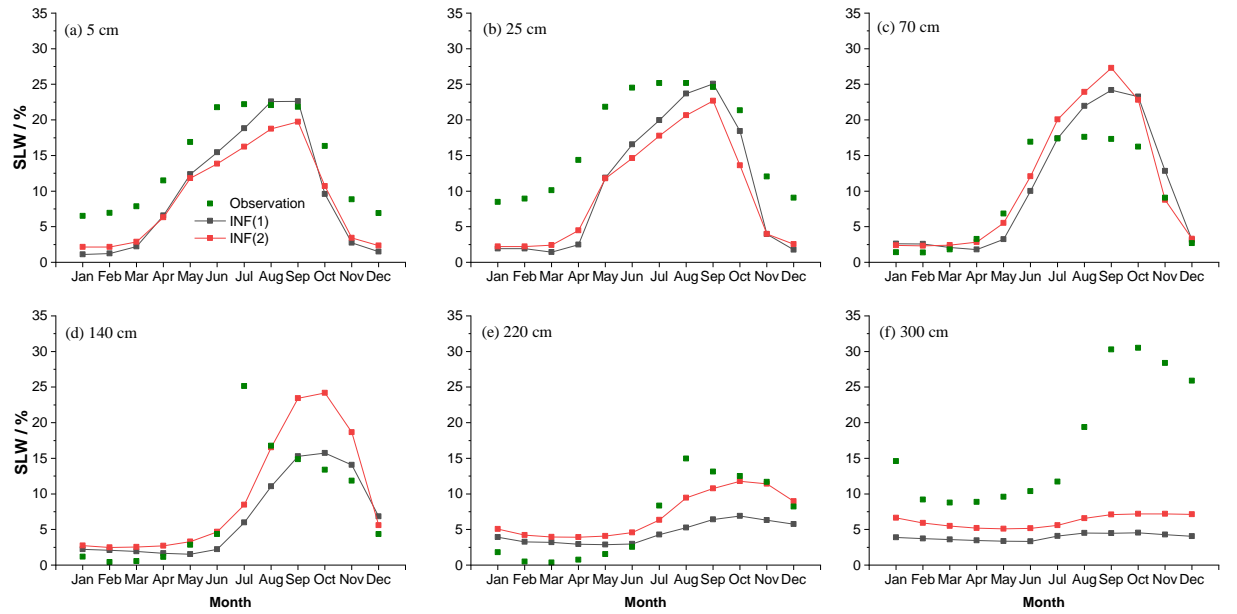


Figure. S3 Monthly soil liquid water (SLW in %) at (a) 5 cm, (b) 25 cm, (c) 70 cm, (d) 140 cm, (e) 220 cm, (f) 300 cm for the INF process.

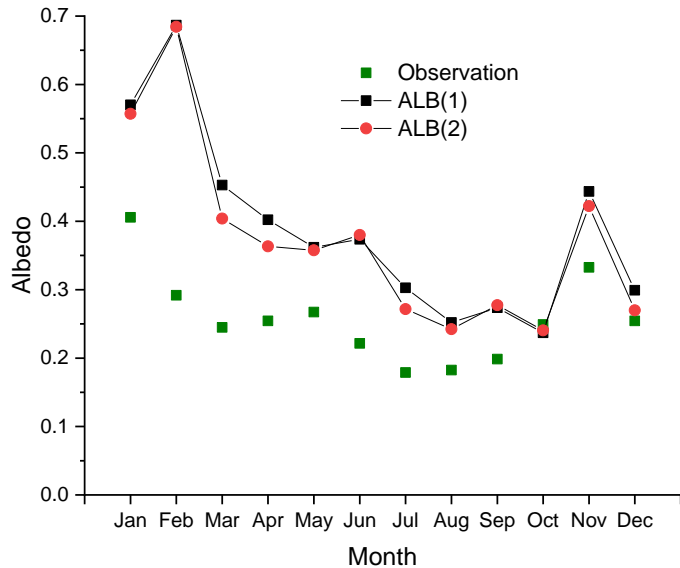


Figure. S4 Monthly ground albedo for the ALB process.

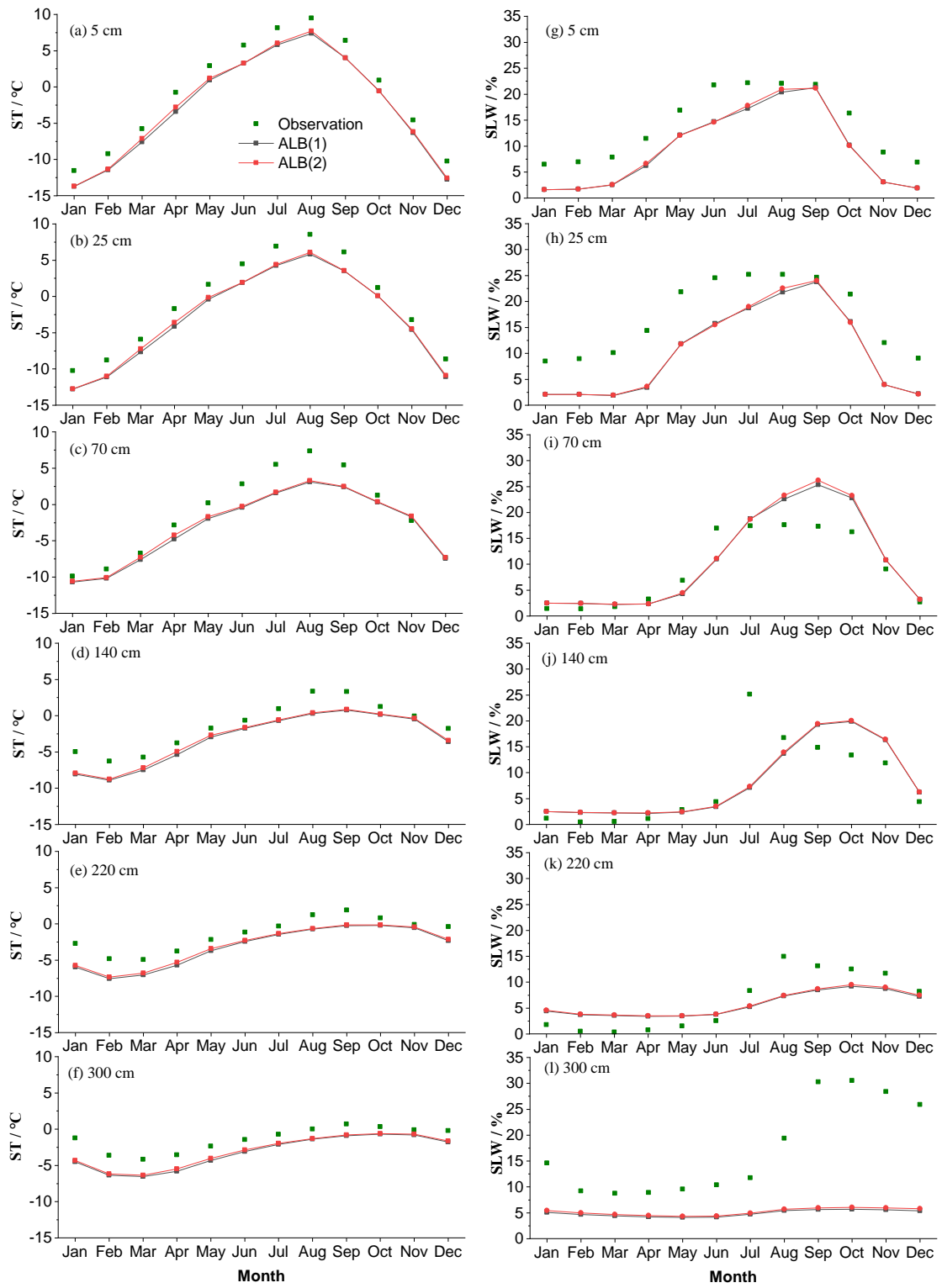


Figure. S5 Monthly soil temperature (ST in °C) and liquid water (SLW in %) at (a, g) 5 cm, (b, h) 25 cm, (c, i) 70 cm, (d, j) 140 cm, (e, k) 220 cm, (f, l) 300 cm for the ALB process.

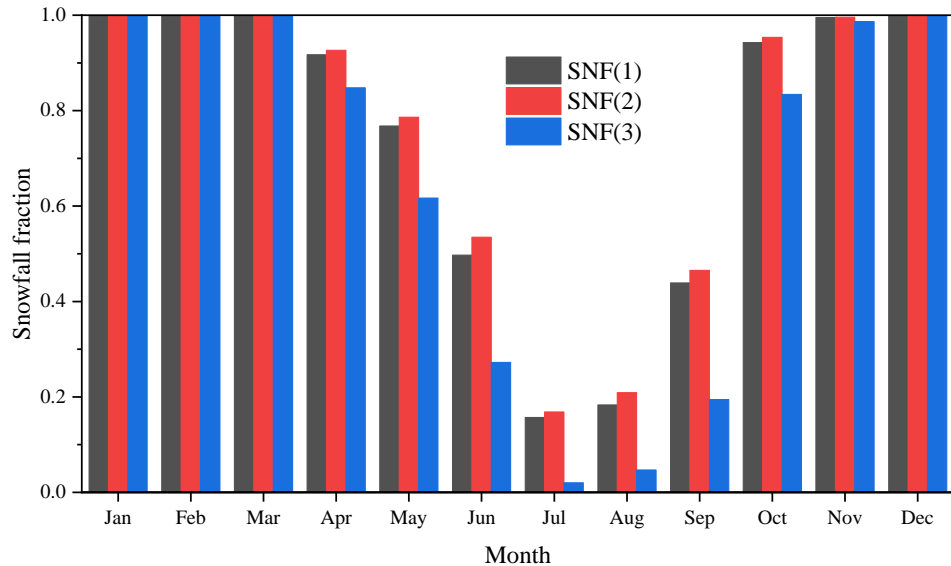


Figure. S6 Monthly snowfall fraction for the SNF process.

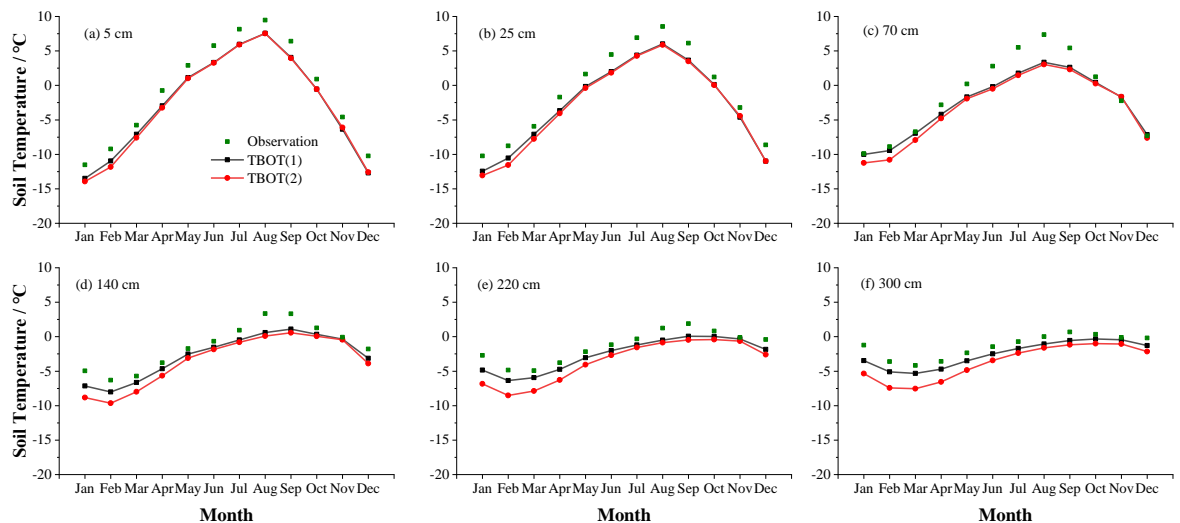


Figure. S7 Monthly soil temperature at (a) 5 cm, (b) 25 cm, (c) 70 cm, (d) 140 cm, (e) 220 cm, (f) 300 cm for the TBOT process.

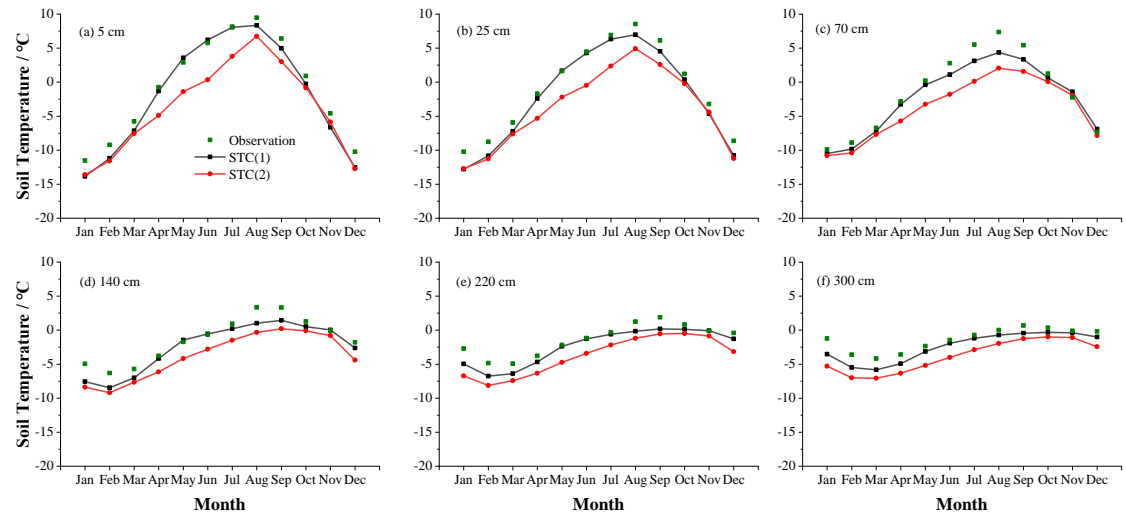


Figure. S8 Monthly soil temperature at (a) 5 cm, (b) 25 cm, (c) 70 cm, (d) 140 cm, (e) 220 cm, (f) 300 cm for the STC process.

Main findings at BLH site:

- (1) Noah-MP tend to overestimate snow cover events at BLH site with large uncertainties during the cold months (Nov.-Mar). Moreover, snow cover events are mostly influenced by the STC and SUB process (Figure S11), and the combination of STC(1) and SUB(2) tend to produce better results (Figure 8). The small influence of physical processes during the warm season (Figure S11c) is because there are limited snow events, and its inability of reproducing snow cover in May (Figure S9).
- (2) Noah-MP generally underestimate STs with relatively large gaps during the snow-affected months (Nov.-Mar.), and the simulated ST in the snow-affected months (Nov.-Mar.) showed relatively wide uncertainty ranges (Figure S10). STs is mostly influenced by the snow processes, i.e. the STC and SUB process (Figure S12), especially during the cold season. In the warm season, the SFC and RUN process dominate the simulation of STs (Figure S12c). The combination of roughness length for heat and under-canopy aerodynamic resistance contributes to elevated soil temperature (Figure S17).
- (3) Noah-MP totally underestimate SLW at BLH site (Figure S10). The RUN process dominates the SLW at most layers simulation with limit impacts (Figure S12).

- General performance of the ensemble simulation

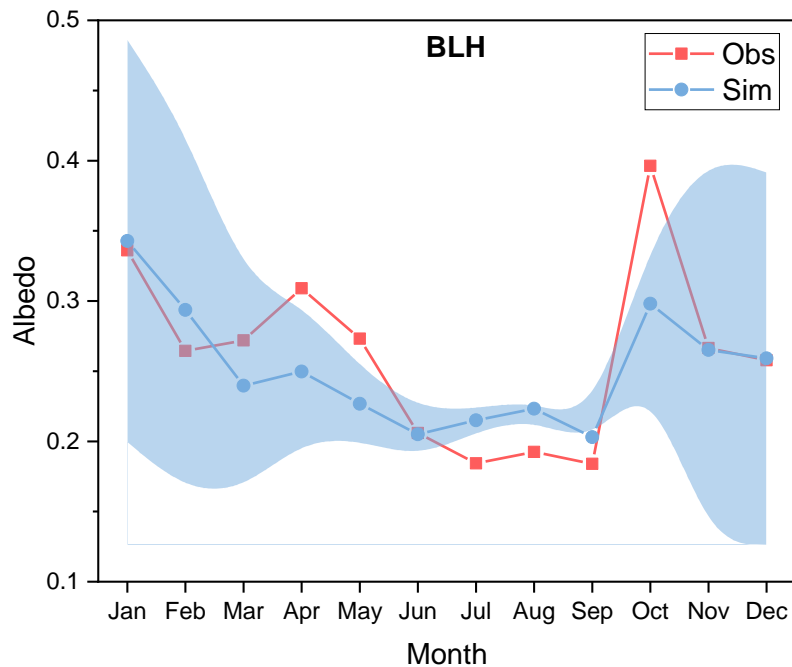


Figure S9. Monthly variations of ground albedo at BLH site for observation (Obs), and the ensemble simulation (Sim). The light blue shadow represents the standard deviation of the ensemble simulation.

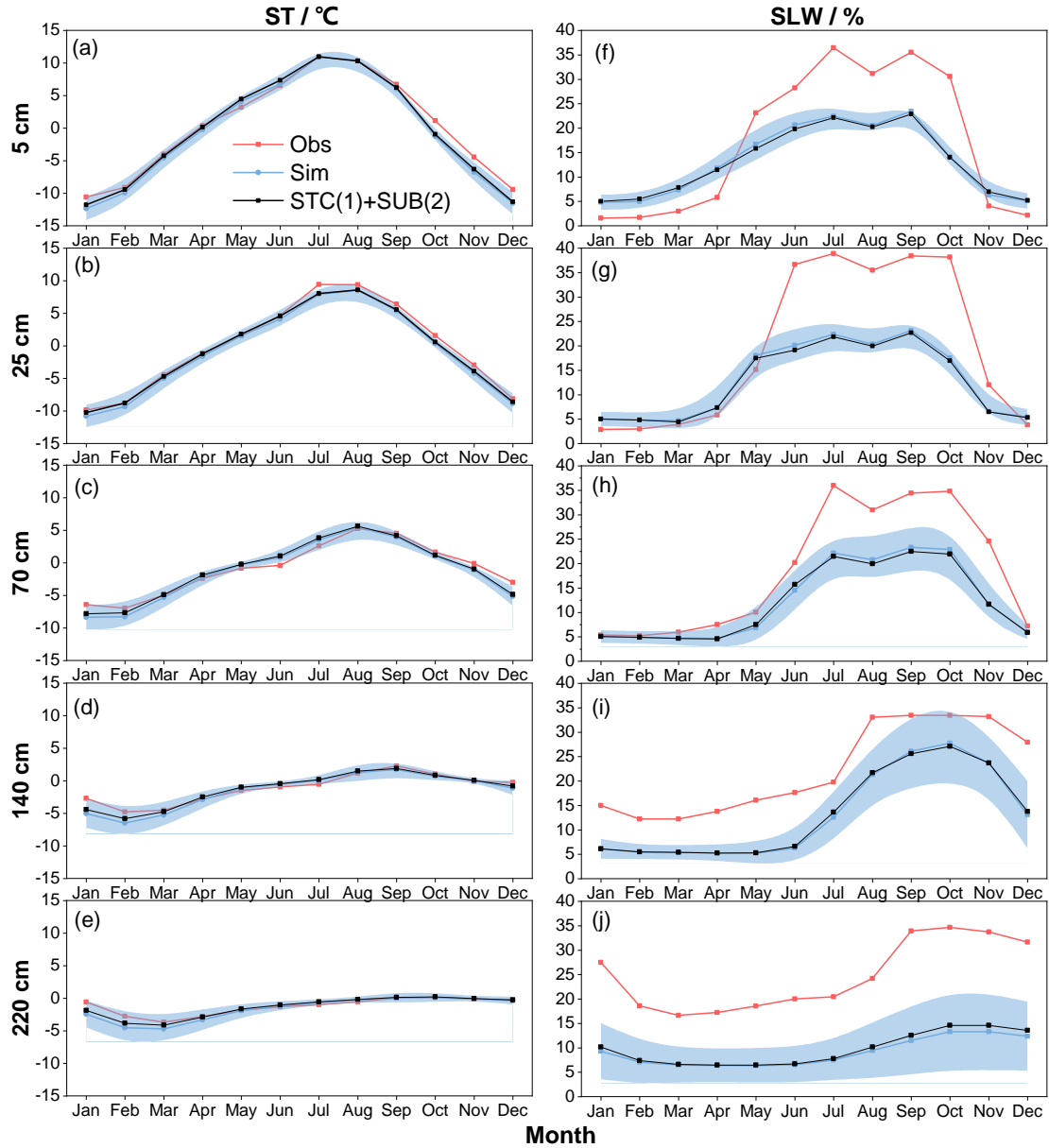


Figure S10. Monthly soil temperature (ST in °C) and soil liquid water (SLW in %) at (a, g) 5 cm, (b, h) 25 cm, (c, i) 70 cm, (d, j) 140 cm, (e, k) 220 cm, (f, l) 300 cm at BLH site. The light blue shadow represents the standard deviation of the ensemble simulation. The black line-symbol represents the ensemble mean of simulations with STC(1) and SUB(2).

- Influence degrees of physical processes

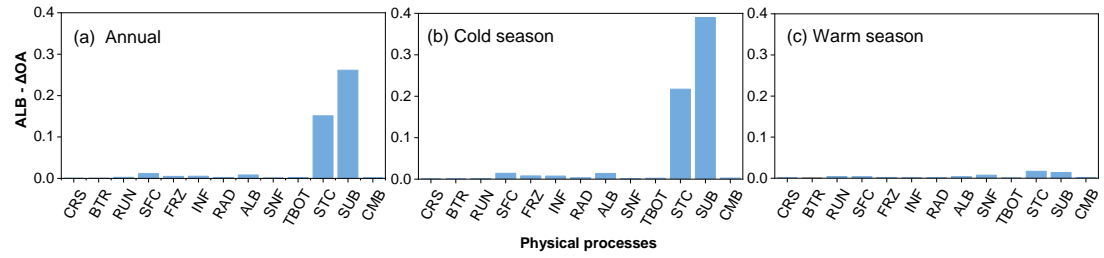


Figure S11. The maximum difference of the mean overall accuracy (OA) for albedo ($ALB - \Delta OA$) in each physical process during the (a) annual, (b) cold season, and (c) warm season at BLH site.

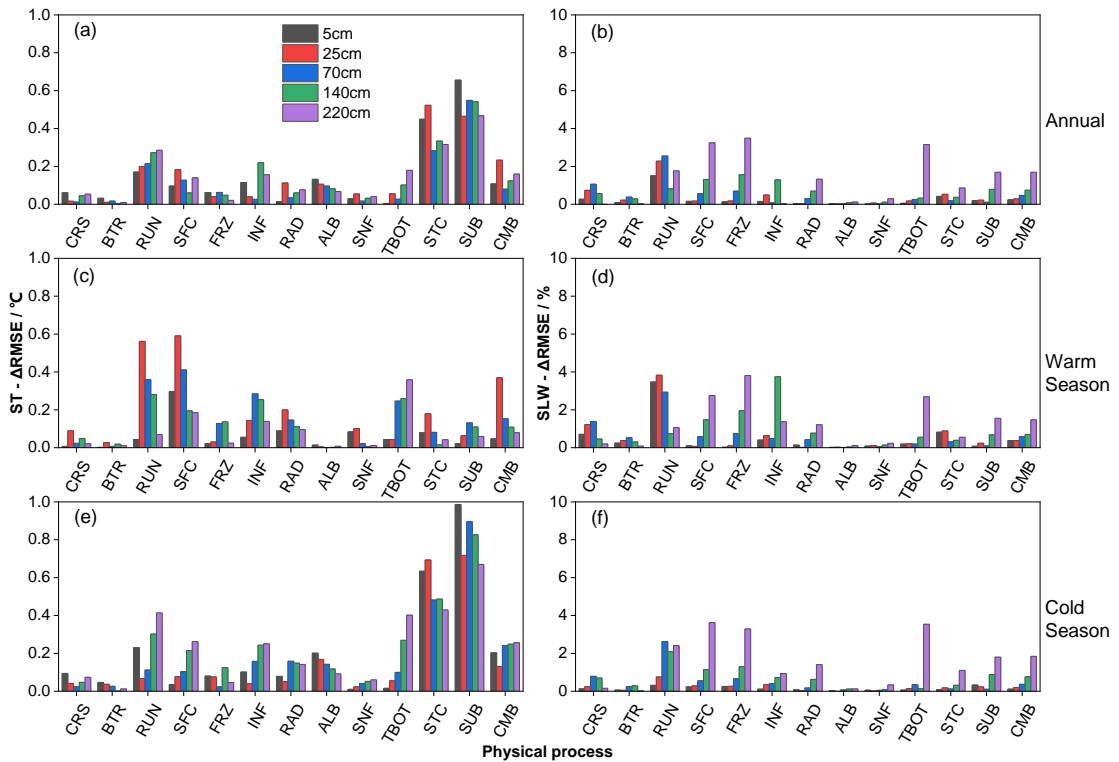


Figure S12. The maximum difference of the mean RMSE for (a, c and e) soil temperature ($ST - \Delta RMSE$ in °C) and (b, d and f) soil liquid water ($SLW - \Delta RMSE$ in %) in each physical process during the (a and b) annual, (c and d) warm, and (e and f) cold season at different soil depths at BLH site.

- Sensitivities of physical processes and general behaviors of parameterizations

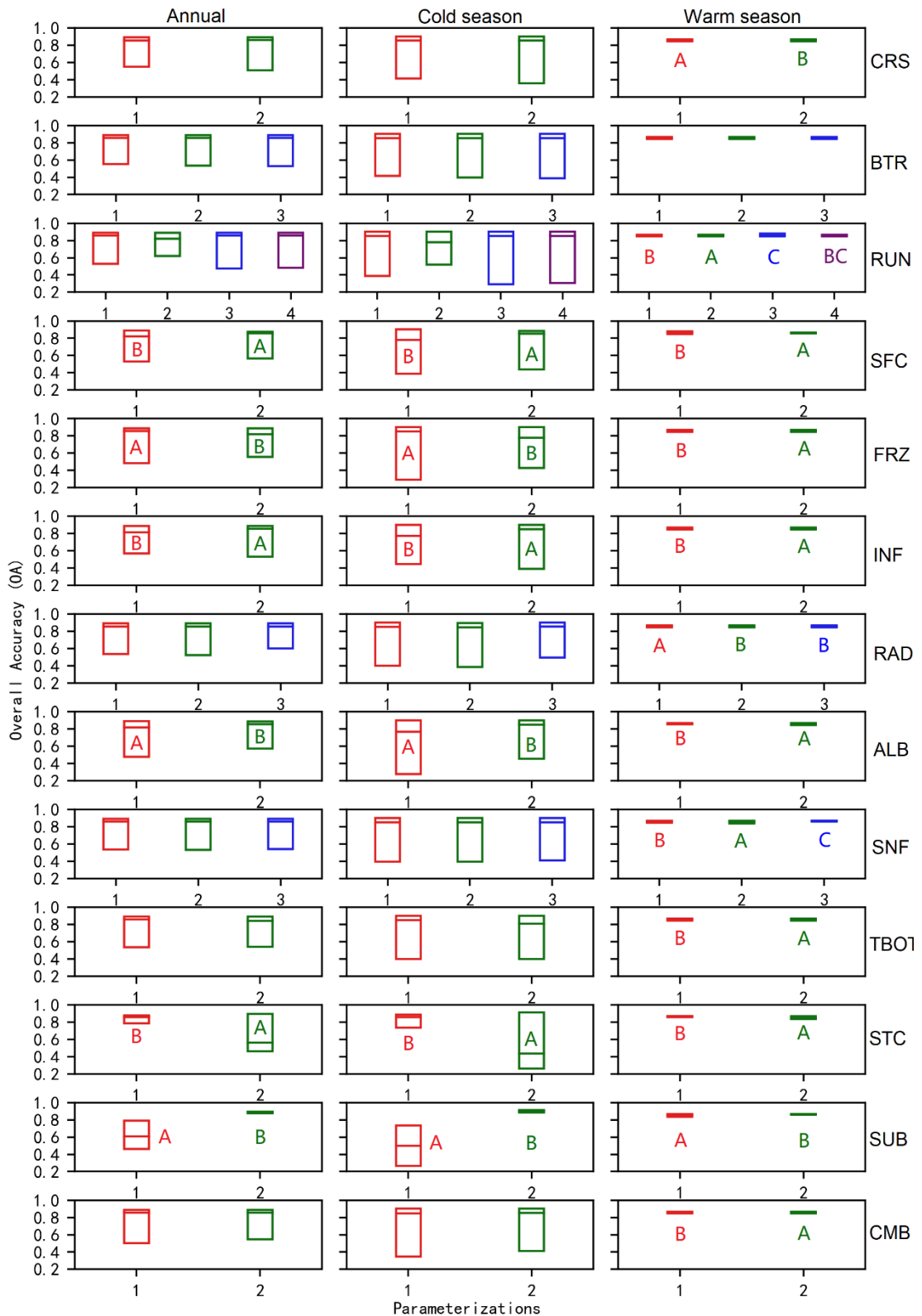


Figure S13. Distinction level for overall accuracy (OA) of snow cover events (SCEs) during the annual, warm, and cold seasons in the ensemble simulations at BLH site.

Limits of the boxes represent upper and lower quartiles, lines in the box indicate the median value.

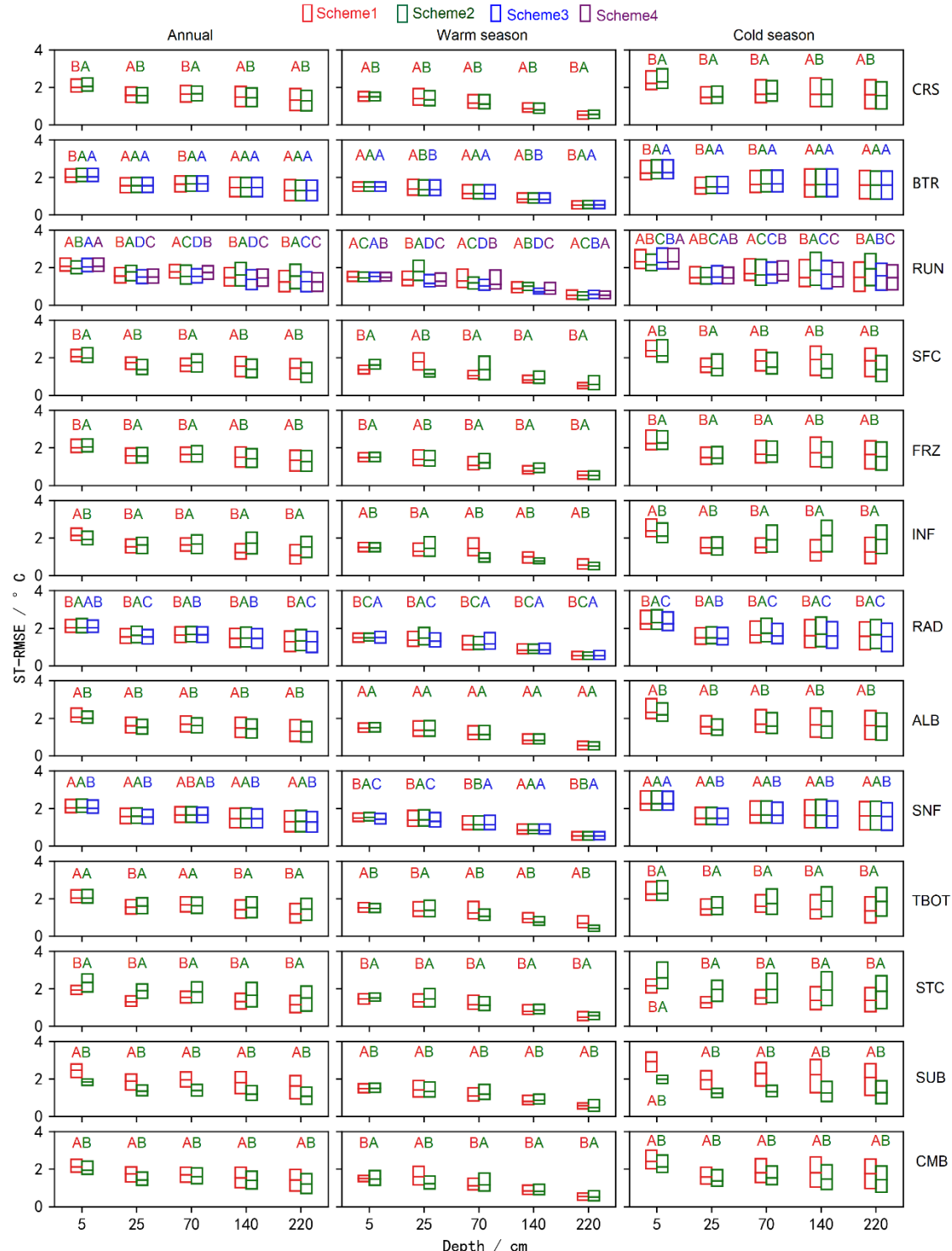


Figure S14. Distinction level for RMSE of ST at different layers during the annual, warm, and cold seasons in the ensemble simulations at BLH site. Limits of the boxes represent upper and lower quartiles, lines in the box indicate the median value.

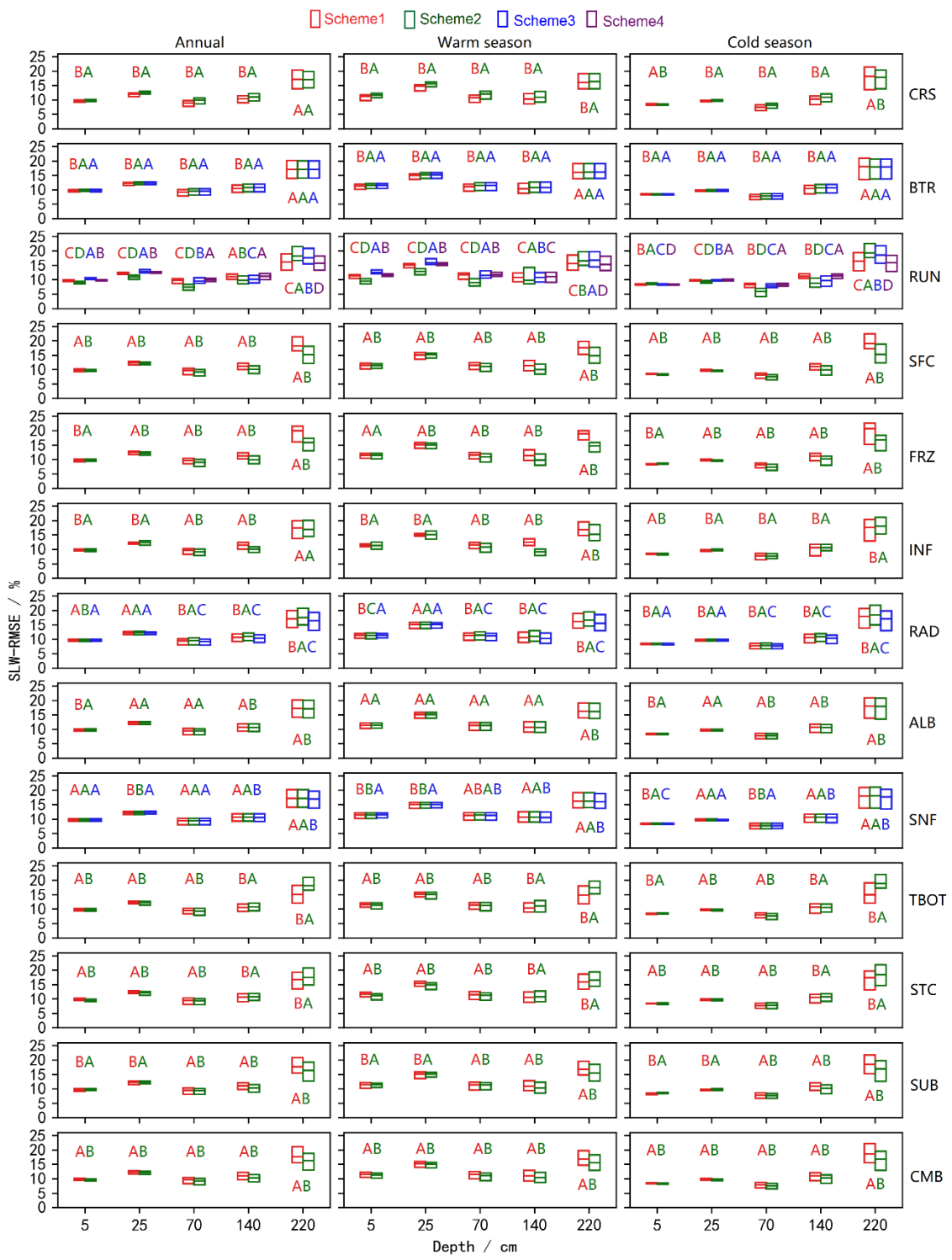


Figure S15. Distinction level for RMSE of SH2O at different layers during the annual, warm, and cold seasons in the ensemble simulations at BLH site. Limits of the boxes represent upper and lower quartiles, lines in the box indicate the median value.

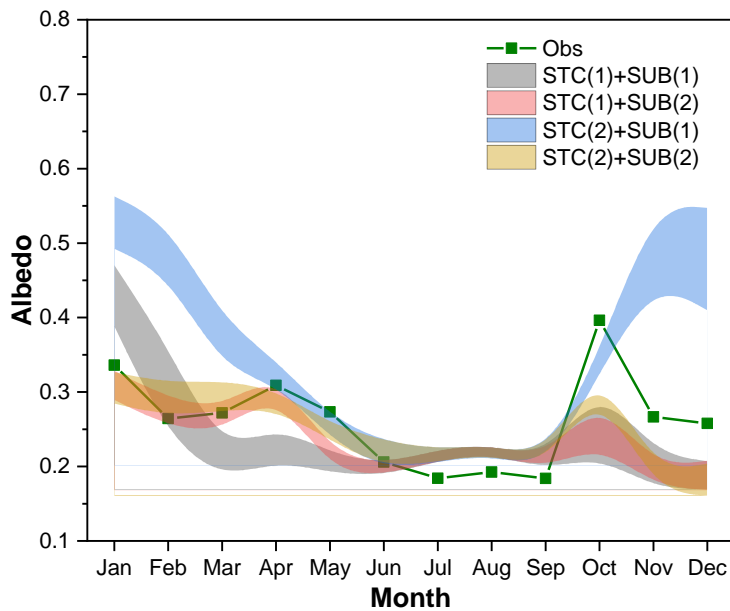


Figure S16. Uncertainty interval of ground albedo at BLH site in dominant physical processes (STC and SUB) for snow cover event simulation.

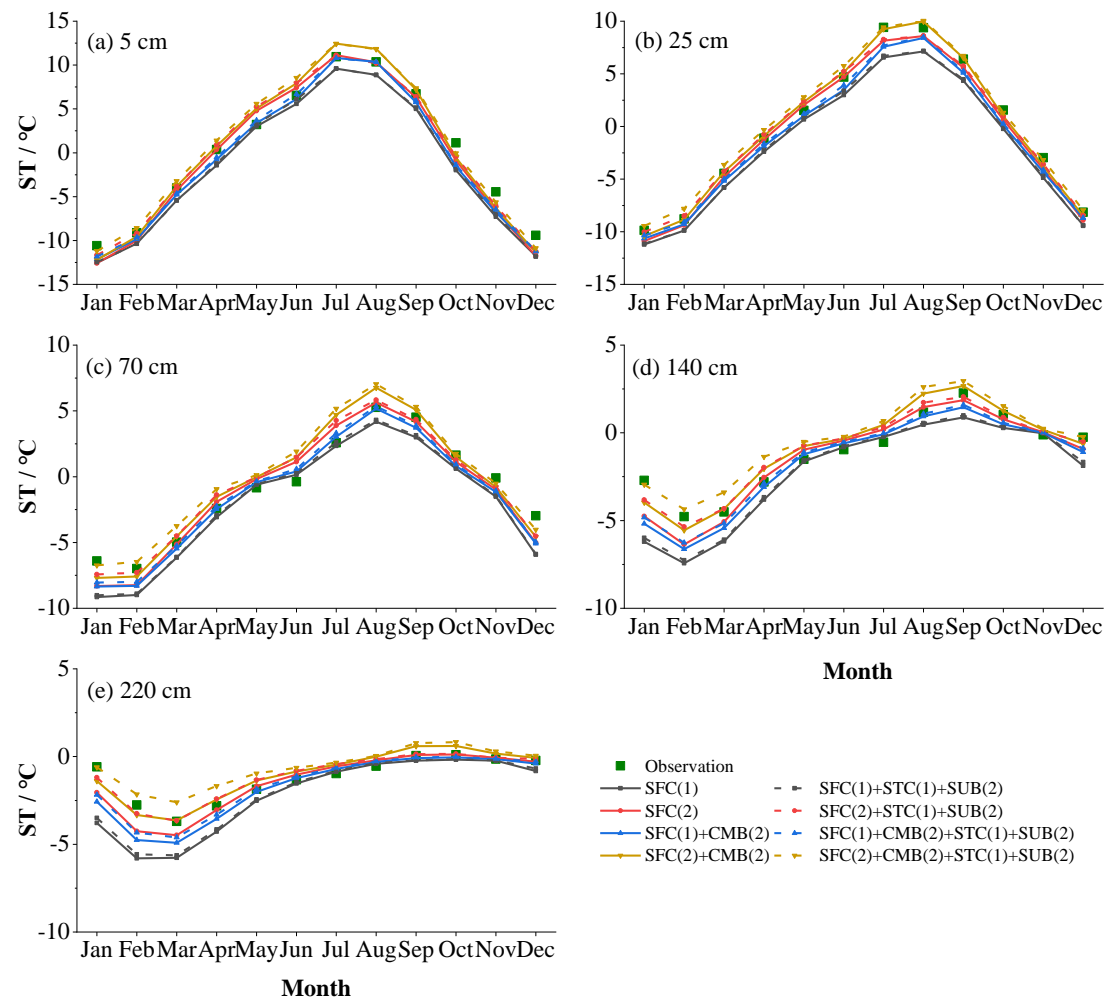


Figure S17. Monthly soil temperature (ST in °C) at (a) 5 cm, (b) 25 cm, (c) 70 cm, (d)

140 cm, (e) 220 cm, (f) 300 cm for the SFC process that consider the CMB(2) and STC(1)+SUB(2) processes or not.

References:

- Hillel, D.: Applications of Soil Physics, Academic Press, 400 pp., 1980.
- Cosby, B. J., Hornberger, G. M., Clapp, R. B., and Ginn, T. R.: A Statistical Exploration of the Relationships of Soil Moisture Characteristics to the Physical Properties of Soils, Water Resour. Res., 20, 682-690, <https://doi.org/10.1029/WR020i006p00682>, 1984.
- Wetzel, P., and Chang, J.-T.: Concerning the Relationship between Evapotranspiration and Soil Moisture, J. Clim. Appl. Meteorol., 26, 18-27, [https://doi.org/10.1175/1520-0450\(1987\)026<0018:CTRBEA>2.0.CO;2](https://doi.org/10.1175/1520-0450(1987)026<0018:CTRBEA>2.0.CO;2), 1987.